Thermotropic Hydrocarbon Side-Chain Liquid-Crystalline Polymers. 3. Characterization of Liquid-Crystalline Phases

Joseph J. Mallon[†] and Simon W. Kantor*

Department of Polymer Science and Engineering, Materials Research Laboratory, University of Massachusetts, Amherst, Massachusetts 01003. *Received March 16, 1989; Revised Manuscript Received August 31, 1989*

ABSTRACT: A series of seven new hydrocarbon polymers with biphenyl mesogens have been characterized via differential scanning calorimetry (DSC), X-ray diffraction of fibers and powders, and polarized-light optical microscopy (POM). The polymers consist of a biphenyl mesogen attached to a polyethylene backbone via four- or six-carbon alkylene spacer groups with H, ethyl, or *n*-butyl terminal groups or tails. The polymers without tails were not liquid crystalline, and the polymers with tails were liquid crystalline. The liquid-crystalline polymers displayed smectic E and smectic B phases. The new liquid-crystalline polymers are more closely related to long side-chain poly(1-alkene)s than to more traditional poly(siloxane) and poly(acrylate) side-chain liquid-crystalline polymers. Four-carbon tails were more effective than two-carbon tails for stabilizing the mesophase. The ability of the tail to stabilize the mesophase closely parallels the effect of the tails for monomers and model compounds. The tail apparently increases the effective axial ratio of the mesogen, resulting in liquid-crystalline behavior.

Introduction

A compilation of thermotropic hydrocarbon liquid crystals obtained in a recent search of the literature has been previously published.[1,2] In most cases, the reported liquid crystals were synthesized to compare their properties to other liquid crystals containing polar or hydrogen-bonding functionalities. Few authors explicitly discuss hydrocarbon liquid crystals as a separate class of mesogenic molecules. The most notable exceptions are the works of Osman[3] and Toyne,[4] who point out that hydrocarbon liquid crystals have very weak intermolecular attractions yet retain their liquid-crystalline character because of their anisotropic shape. Samulski and Toriumi have suggested[5] that 4,4-di-*n*-alkylbicyclo[2.2.0]octanes have especially low intermolecular attractions and would thus be useful for the comparison of various theories of the liquid-crystalline phase. Others have expressed interest[6-8] in hydrocarbon liquid crystals because of their low viscosities. Varech and Jacques have also explored[9] the importance of geometrical factors for the stability of the liquid-crystalline phase by studying hydrocarbon systems.

The only hydrocarbon side-chain liquid-crystalline polymers that have been reported are poly(1-alkene)s. A comprehensive review of the field of polymers with long paraffinic side groups has been published by Plate and Shibaev.[10] In 1964 Turner Jones proposed[11] that poly(1-alkene)s with long side chains formed layered structures above their crystalline melting temperatures. Her X-ray data showed two diffraction maxima for each amorphous polymer. One diffraction maximum corresponded to a *d*-spacing of ~4.65 Å and was attributed to the spacing between side chains. The other diffraction maximum was at a higher spacing and varied linearly with the number of carbon atoms in the side chain. She also showed that the crystal structures of poly(1-alkene)s below their crystalline melting points were very dependent on crystallization conditions.

A series of experiments by Magagnini et al. has demonstrated[12-15] the importance of heating effects and tacticity on the crystal structure of poly(1-eicosene). The poly(1-eicosene) was prepared with $TiCl_3/Al(i\text{-}Bu)_3$ to yield a mixture of atactic and isotactic polymers. The fractions were separated by solvent extraction and characterized by infrared (IR) spectroscopy, nuclear magnetic resonance (NMR) spectroscopy, differential scanning calorimetry (DSC), and X-ray diffraction. In summary, his results showed that the unexpected polymer has two melting points, corresponding to the melting points of the incompatible atactic and isotactic fractions. When the fractions are separated, the lower melting is the atactic polymer and the higher melting fraction is isotactic. A study of the temperature dependence of the crystal structure shows that the side-chain packing of both fractions is orthorhombic at lower temperatures and hexagonal at higher temperatures. At any given temperature, a larger proportion of the isotactic fraction is orthorhombic relative to the atactic fraction. The orthorhombic–hexagonal transition takes place on heating in both fractions over a broad temperature range. The transition range is different in size and temperature for each fraction. The transition is undetectable by normal DSC methods, in contrast to the orthorhombic–hexagonal transition in linear paraffins with $n > 22$, which is readily detectable by DSC. The X-ray diffraction data[14] show that both fractions can display liquid-crystalline structures depending on the annealing conditions.

In the first paper of this series,[16] we reported the synthesis and characterization of a new series of monoalkyl- and dialkyl-substituted biphenyl monomers. Dialkyl substitution of the biphenyl mesogen was shown to be necessary for the formation of a liquid-crystalline phase. The liquid-crystalline monomers had isotropization or clearing temperatures between 26 and 42 °C and exhibited smectic B phases (hexagonal packing within smectic layers).

The monomers were polymerized through terminal carbon–carbon double bonds with Ziegler–Natta catalysts. The resulting polymers used in our study were polyethylenes substituted at every other carbon atom with a flexible spacer connected to a biphenyl mesogenic unit as represented in 1. The flexible spacer consisted of either four or six methylene units ($m = 4$ or 6). The biphenyl moiety was either unsubstituted in the second ring para position ($n = 0$) or substituted with an ethyl group ($n = 2$) or an *n*-butyl group ($n = 4$). These para substituted

[†] Present address: The Aerospace Corp., Los Angeles, CA 90009.

0024-9297/90/2223-1249$02.50/0

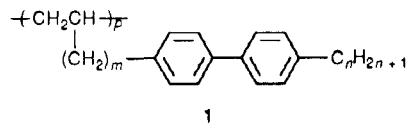

1

groups are referred to as terminal groups or tails. The syntheses and characterization of the polymers, their molecular weights, and tacticities were reported in the second publication in this series.[17] The molecular weights of the polymers were high (M_w = 250 000–850 000) with broad molecular weight distributions (5–24) as measured by gel permeation chromatography (polystyrene standards). The tacticities of the polymers were measured using high-field ^{13}C NMR and ranged from 65% to 90% isotactic.

In the present work the liquid-crystalline properties of the new polymers are characterized by DSC, polarized-light optical microscopy (POM), and X-ray diffraction of fibers and powders. The influence of tail and spacer length on the properties is discussed. The liquid-crystalline properties are compared to other poly(1-alkene)s.

Experimental Section

The syntheses of the polymers have been described previously.[17]

Measurements. DSC experiments were performed on a Perkin Elmer DSC-II at a heating rate of 20 °C/min and a cooling rate of 10 °C/min, except where noted. The instrument was calibrated with standard samples of indium and naphthalene. To ensure that all of the samples had equivalent thermal histories, the results of the second heating scan have been reported throughout.

POM studies were carried out on a Leitz–Wetzler microscope equipped with a Mettler hot stage at a magnification of 320×. Photomicrographs were taken at a magnification of 120× with crossed polarizers.

X-ray diffraction experiments were carried out on a Statton flat film camera using Ni-filtered Cu Kα radiation. The polymer samples (either powders or melt-drawn fibers) were sealed in glass capillaries and placed into a homemade hot stage. Powder samples were heated above their respective clearing temperatures and then cooled to room temperature to ensure that all of the samples had equivalent thermal histories.

A typical experiment consisted of three 1-h exposures for each fiber or powder sample. The first exposure was done at room temperature, the second about 10 °C below the clearing temperature, and the third at room temperature again.

Results and Discussion

The data obtained from the results of the DSC experiments are summarized in Table I. The systematic names of the polymers are rather awkward, so they will be referred to by the code names shown in Table I. The code names are identical to those used in the second paper of this series.[17] The polymers were prepared with $Et_3Al/TiCl_4$ catalyst except for PEBP26 #2, as noted previously.[17]

All of the polymers are brittle at room temperature. When pressure was applied to a sample of polymer that was contained between two glass cover slips and heated on a Fisher-Johns melting point apparatus, all of the polymers were observed to wet the cover slips at a temperature of 60 ± 5 °C. No clear evidence of a glass transition is observed by DSC. The second heating and cooling DSC scans for the seven polymers are shown in Figures 1–7. The transition temperatures reported are for the peak maxima of the second heating scan. All of the polymers exhibited significant supercooling on cooling at 10 °C/min. This behavior is typical for high molecular weight liquid-crystalline polymers and is in contrast to low molecular weight liquid crystals, which usually exhibit little or no supercooling.[18,19] The two non-liquid-crystalline polymers, PEBPO4 and PEBPO6, showed extensive supercooling of their crystalline melting peaks, 56 and 36 °C, respectively. Table II contains the data obtained from the second and third exposures of the fiber X-ray exper-

Table I
Polymer Thermal Properties

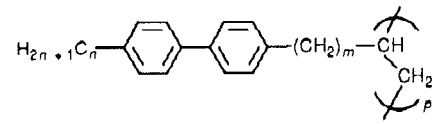

code[a]	n	m	transition temp,[b] °C
PEBPO4	0	4	K 151 I
PEBPO6	0	6	K 126 I
PEBP24	2	4	S_E broad S_B S_B 197 I
PEBP26 #1	2	6	S_E broad S_B S_B 176 I
PEBP 26 #2	2	6	S_E broad S_B S_B 176 I
PEBP44	4	4	S_E 158 S_B S_B 206 I
PEBP46	4	6	S_E 145 S_B S_B 181 I

[a] PE = polyethylene (backbone), BP = biphenyl mesogen, first digit after P = n, second digit after P = m. [b] ΔH and ΔS have not been reported due to the broad nature of the S_E to S_B transition and the resulting uncertainty in using the proper base line.

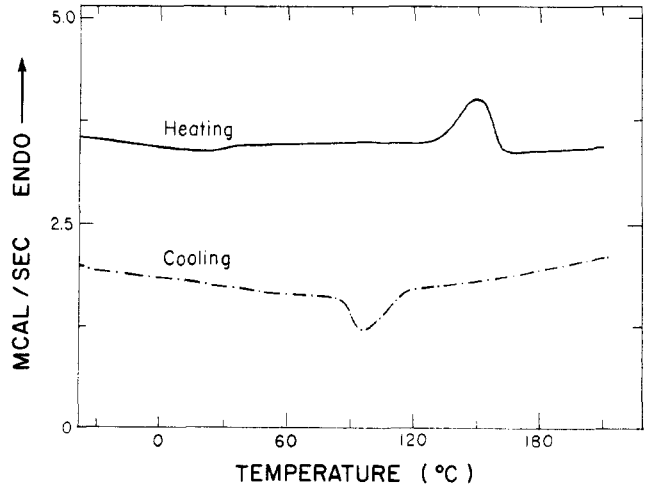

Figure 1. Second heating and cooling DSC scans for PEBO4 (described in Table I). Heating rate: 20 °C/min. Cooling rate: 10 °C/min.

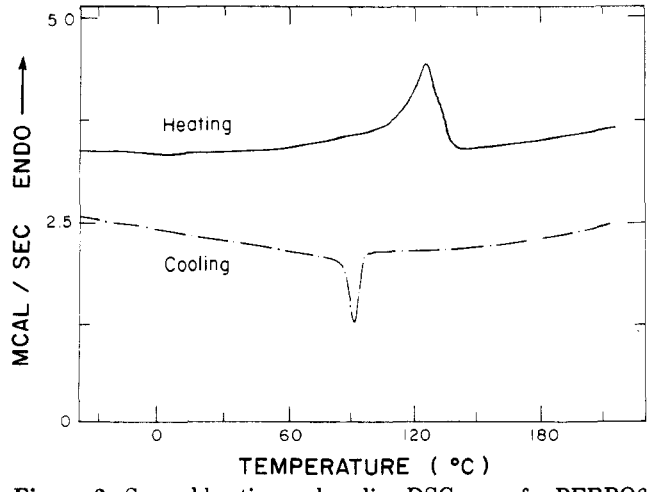

Figure 2. Second heating and cooling DSC scans for PEBPO6 (described in Table I). Heating rate: 20 °C/min. Cooling rate: 10 °C/min.

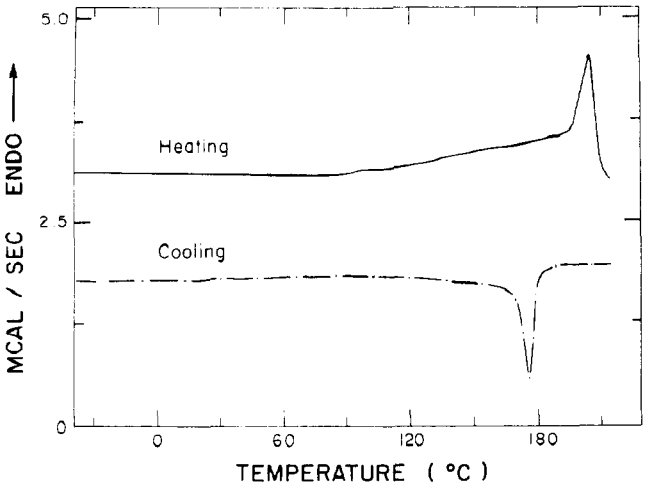

Figure 3. Second heating and cooling DSC scans for PEBP24 (described in Table I). Heating rate: 20 °C/min. Cooling rate: 10 °C/min.

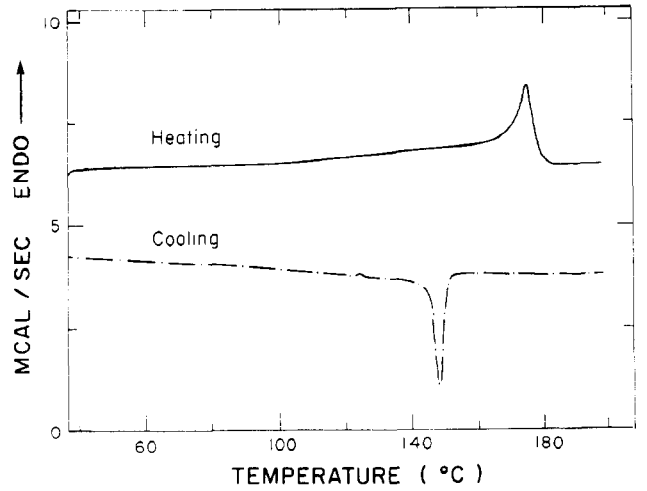

Figure 4. Second heating and cooling DSC scans for PEBP26 #1 (described in Table I). Heating rate: 20 °C/min. Cooling rate: 10 °C/min.

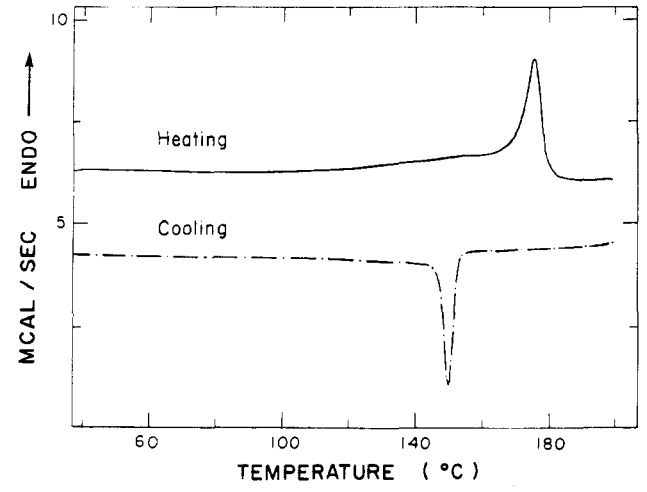

Figure 5. Second heating and cooling DSC scans for PEBP26 #2 (described in Table I). Heating rate: 20 °C/min. Cooling rate: 10 °C/min.

iments. PEBP26 #1 and PEBP26 #2 gave identical results so their X-ray data have been combined. The *d*-spacings are given in angstroms, and the letters in parentheses after the values are the intensities and positions of the reflections. The abbreviations vs = very strong, s = strong, m = medium, w = weak, and vw = very weak

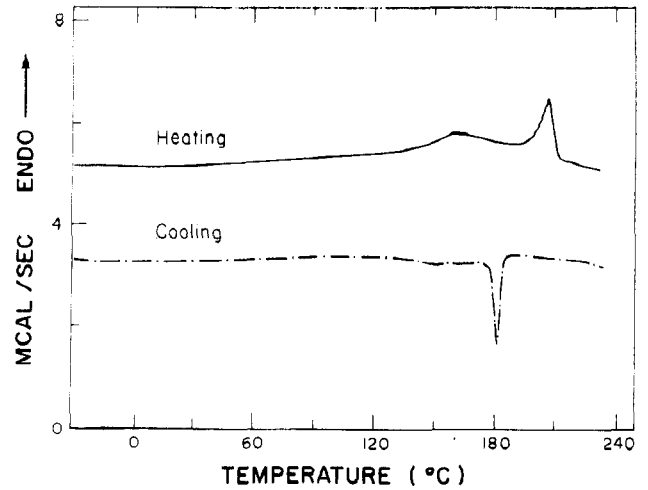

Figure 6. Second heating and cooling DSC scans for PEBP44 (described in Table I). Heating rate: 20 °C/min. Cooling rate: 10 °C/min.

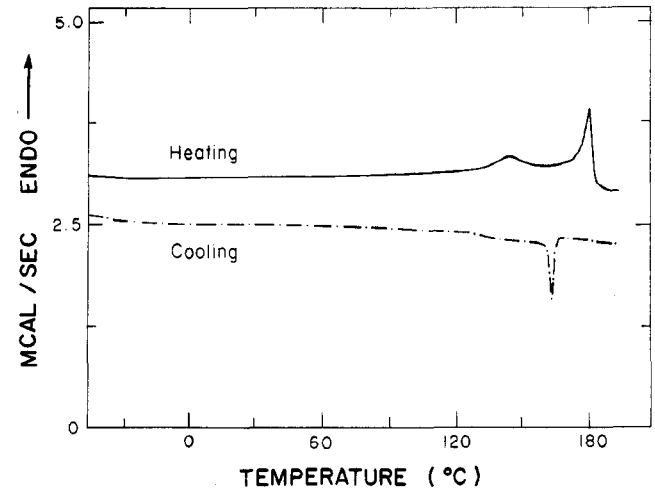

Figure 7. Second heating and cooling DSC scans for PEBP46 (described in Table I). Heating rate: 20 °C/min. Cooling rate: 10 °C/min.

describe the intensities. The positions of the rings or arcs are described as h = halo (ring) or e = equatorial (arc). No meridional arcs were observed for any of the fiber patterns.

The DSC scans for PEBPO4 and PEBPO6 both show a broad transition on heating or cooling that corresponds to the crystalline melting temperature as observed by POM. Characteristic liquid-crystalline textures were not observed by POM for PEBPO4 or PEBPO6. The X-ray diffraction patterns of a melt-drawn fiber sample of PEBPO4 at 145 and 27 °C are shown in Figure 8. The X-ray diffraction patterns obtained for PEBPO6 are very similar. The small-angle equatorial arcs correspond to a Bragg maximum of d = 28 Å for PEBPO4. This layer spacing corresponds to a double layer type of packing in which the side groups are arranged on both sides of the main chain.[20,21] The wide-angle halo corresponds to an intermolecular spacing of 4.7 Å. Wide-angle equatorial arcs are also present, corresponding to Bragg maxima at d = 6.3 and 4.0 Å. These wide-angle equatorial arcs are sharper in the 27 °C sample and more diffuse at 145 °C, indicating that the polymer becomes more ordered as it cools. The wide-angle equatorial arcs result from some structural regularity in a direction perpendicular to the main chain, possibly crystallization of the polymer backbones with one another. These observations, taken in

Table II
X-ray Fiber Diffraction Data

code	temp, °C	*d*-spacings, Å			
PEBPO4	145	14.0 (vs, e), 6.3 (w, e)	9.3 (vs, e), 4.7 (vs, h)	4.0 (m, e)	
	27	13.9 (vs, e), 6.0 (w, e)	9.2 (vs, e), 4.7 (vs, h)	4.0 (m, e)	3.2 (vw, h)
PEBPO6	120	16.8 (m, e)	11.2 (vs, e), 4.7 (vs, h)	4.2 (m, e)	
	27	16.6 (m, e)	11.0 (vs, e), 4.7 (vs, h)	4.2 (m, e)	6.7 (vw, e), 3.3 (w, h)
PEBP24	185	16.0 (vs, e)	10.6 (vs, e), 4.6 (vs, h)		6.4 (vw, e)
	27	16.0 (vs, e)	10.6 (vs, e), 4.6 (vs, h)		6.4 (vw, e), 3.3 (vw, h)
PEBP26	165	18.8 (vs, e)	12.6 (vs, e), 4.6 (vs, h)		7.4 (w, e)
	27	18.8 (vs, e)	12.6 (vs, e), 4.6 (vs, h)		7.4 (w, e), 3.3 (vw, h)
PEBP44	195	17.9 (vs, e)	11.9 (vs, e), 4.6 (vs, h)	8.9 (vw, e)	7.1 (w, e)
	27	18.0 (vs, e)	11.9 (vs, e), 4.6 (vs, h)	9.0 (w, e)	7.1 (w, e), 3.3 (vw, h)
PEB46	175	19.9 (vs, e)	13.3 (vs, e), 4.6 (vs, h)	10.0 (vw, e)	7.9 (vw, e)
	27	20.0 (vs, e)	13.3 (vs, e), 4.6 (vs, h)	10.0 (vw, e)	7.9 (vw, e), 3.3 (vw, h)

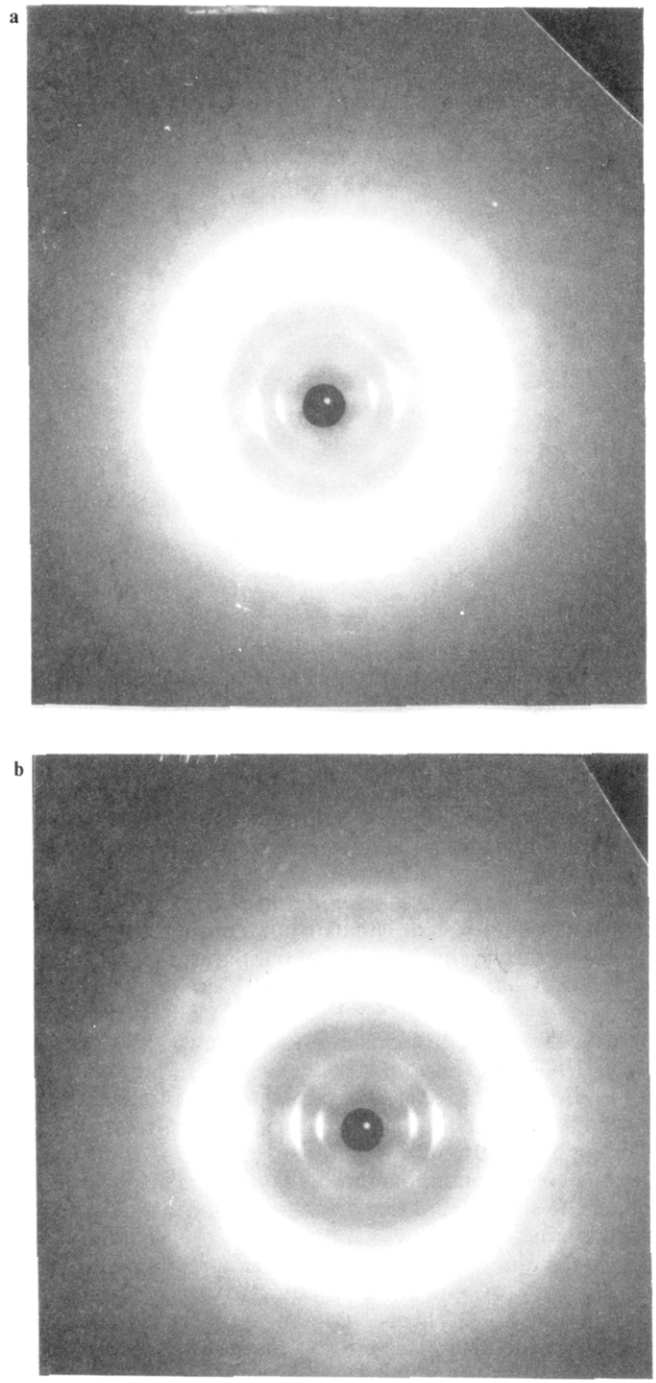

Figure 8. X-ray diffraction patterns of a fiber of PEBPO4 at (a) 145 and (b) 27 °C. The fiber axis is vertical.

combination with the DSC and POM results, indicate that PEBPO4 and PEBPO6 are not liquid crystalline.

The DSC scans of PEBP24, PEBP26 #1, and PEBP26 #2 show a single peak on heating or cooling that corresponds to the isotropization temperature as observed by POM. X-ray diffraction and POM experiments show that these three polymers are liquid crystalline. The X-ray diffraction patterns of a melt-drawn fiber sample of PEBP26 at 165 and 27 °C are shown in Figure 9. The diffraction patterns of PEBP24 are similar. The small-angle equatorial arcs correspond to a Bragg maximum of d = 37 Å. A number of arcs, corresponding to the second-, third-, and fifth-order reflections, can be seen in both polymers. The higher order reflections indicate that the layer spacings in both polymers are highly regular. It is interesting to note that the fourth-order reflections that are expected at 8.0 Å for PEBP24 and 9.3 Å for PEBP26 are absent from the X-ray diffraction patterns. Apparently some structural regularity of the proper repeat distance interferes with the appearance of a fourth-order reflection. The origin of the structural regularity is unknown at this time but correlates with the two-carbon tail. All of the expected higher order reflections are found in the polymers with four-carbon tails discussed below.

The halo seen in the X-ray diffraction patterns shown in Figure 9 at wide angles corresponds to an intermolecular spacing of 4.6 Å, the same intermolecular spacing found for the monomers.[16] At 165 °C, the X-ray diffraction pattern of PEBP26 indicates that it is a smectic B liquid-crystalline polymer. As the polymer is cooled to 27 °C, another diffraction maximum appears at 3.3 Å. The ratio of 4.6/3.3 is approximately the square root of 2, consistent with the transformation of a smectic B (hexagonal) phase to a smectic E (orthorhombic) phase at lower temperatures. The transition is not manifested as a DSC peak on heating or cooling and thus may be occurring over a broad temperature range. If this is the case, then the similarities between the polymers with two-carbon tails and the aforementioned poly(1-eicosene) polymers investigated by Magagnini are striking.

The DSC scans of PEBP44 and PEBP46 both show two overlapping peaks on heating. The higher temperature peak is well-defined and corresponds to the isotropization temperature as observed by POM. The lower temperature peak is broad and barely discernible on cooling. The X-ray diffraction and POM data discussed below establish that PEBP44 and PEBP46 are liquid-crystalline and that the broad, lower temperature peak represents the enthalpy change associated with the smectic E to smectic B transition. The X-ray diffraction patterns of a melt-drawn fiber sample of PEBP46 are shown in Figure 10 at 175 and at 27 °C. The X-ray diffraction pattern of PEBP46 shows first-, second-, third-, fourth-, and fifth-order small-angle equatorial arcs. These are

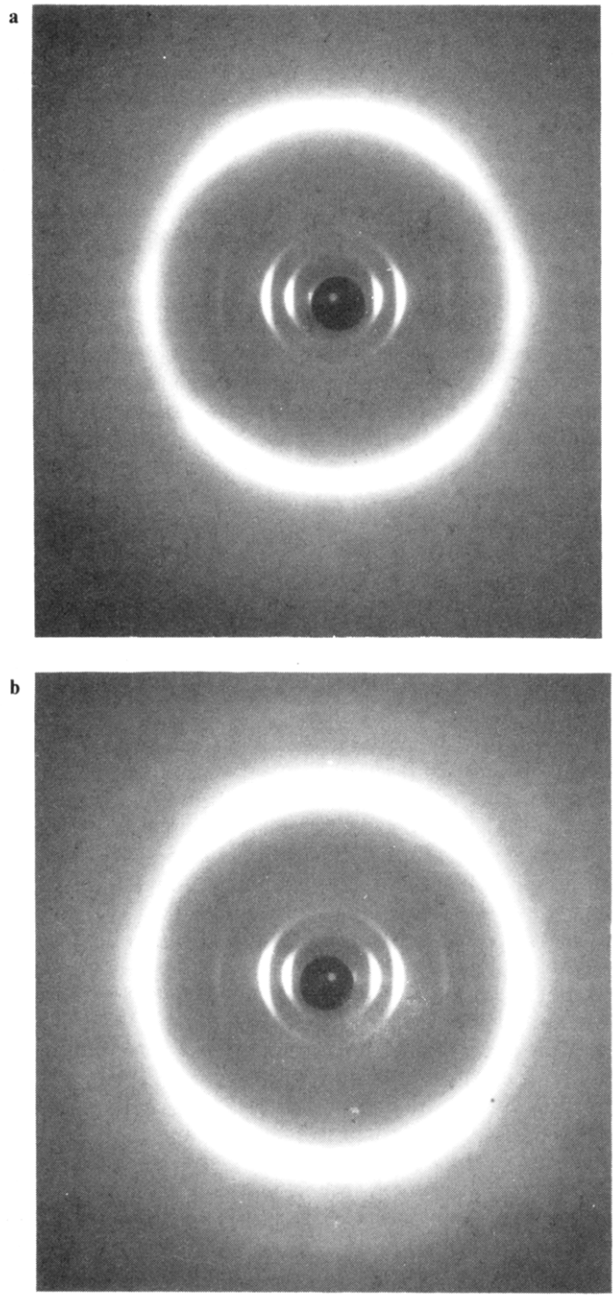

Figure 9. X-ray diffraction pattern of a fiber of PEBP26 at (a) 165 and (b) 27 °C. The fiber axis is vertical.

clearly seen in the small-angle X-ray scattering pattern of a PEBP46 melt-drawn fiber sample shown in Figure 11, confirming the highly ordered layer spacing. The X-ray diffraction patterns obtained for PEBP44 are similar. The wide-angle halo in Figure 10 corresponds to an intermolecular spacing of 4.6 Å, the same spacing as that found for the monomers. The two diffraction patterns in Figure 10 show that another ring corresponding to a Bragg maximum of d = 3.3 Å appears when the fiber sample is cooled from 175 to 27 °C. The ratio 4.6/3.3 is approximately the square root of 2, indicating smectic E (orthorhombic) packing at room temperature and smectic B (hexagonal) packing at higher temperatures. On the basis of the DSC evidence, the transition from smectic E to smectic B occurs at 158 °C for PEBP44 and at 145 °C for PEBP46 on heating. The transition peak is barely discernible on cooling and may occur over a broad temperature range.

POM investigations showed fine-grain textures,[22,23] for the liquid-crystalline polymers that are consistent with

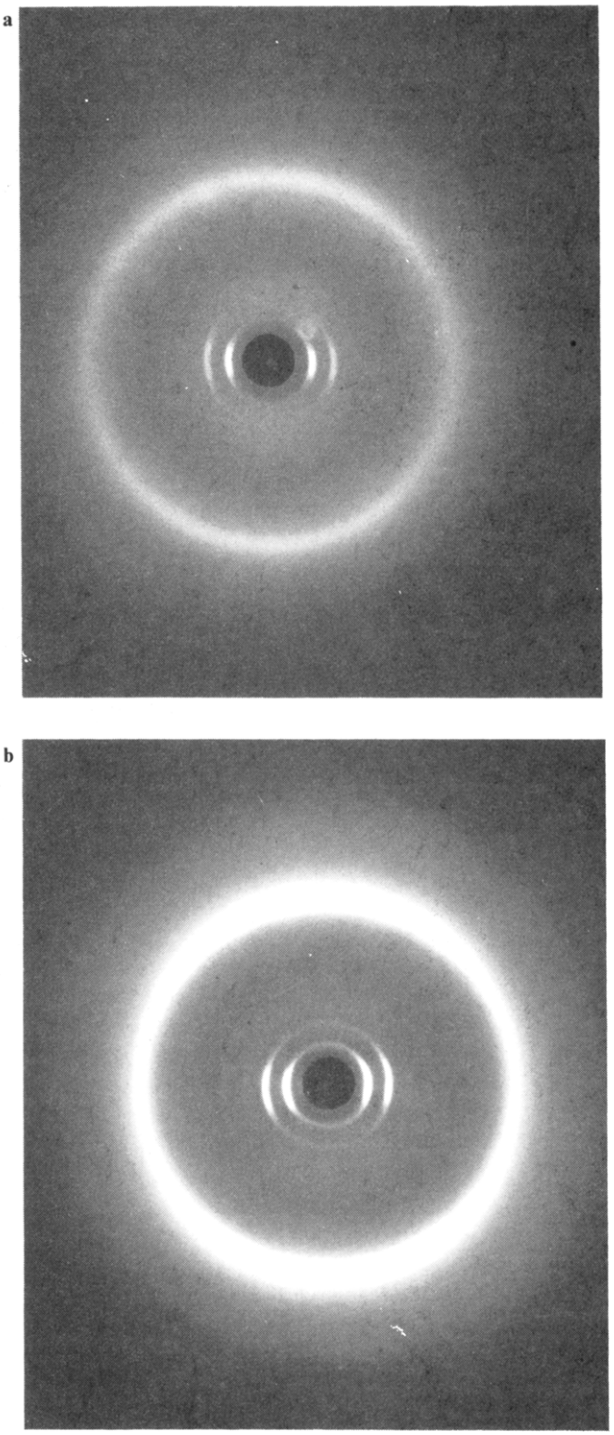

Figure 10. X-ray diffraction patterns of a fiber of PEBP46 at (a) 175 and (b) 27 °C. The fiber axis is vertical.

smectic phases. Annealing the samples at temperatures just below the clearing points for as long as 1 week did not result in more recognizable textures. PEBPO4 and PEBPO6 did not exhibit fine-grain textures. An example of the fine-grain texture exhibited by PEBP46 at 160 °C is shown in Figure 12.

The layer spacings and intermolecular spacings of the four liquid-crystalline polymers are shown in Table III. The layer spacings correspond to a double-layer packing, with the mesogenic groups arrayed on both sides of the main chain. The calculated spacing for double-layer packing shown in Table III was determined by assuming the 2/1 helix structure shown in Figure 13 for PEBP46. The difference between the calculated and observed layer spacing is about 3.5 ± 0.5 Å. The discrepancy is attrib-

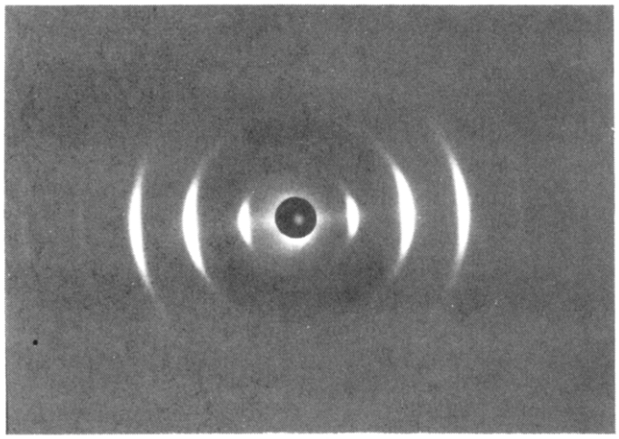

Figure 11. Small-angle X-ray diffraction pattern of a fiber of PEBP46 at 27 °C. The fiber axis is vertical. Five sets of reflections are higher order, first through fifth, corresponding to a *d*-spacing of 40 Å.

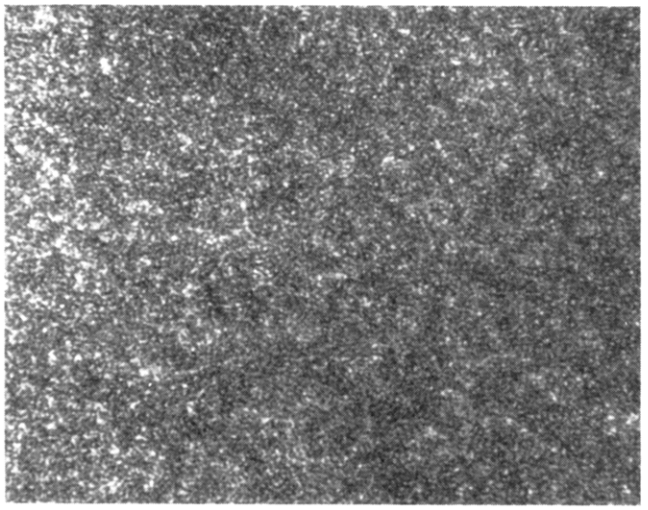

Figure 12. Photomicrograph taken with crossed polarizers at 120× magnification of fine-grain texture exhibited by PEBP46 at 100 °C on cooling.

Table III
Summary of X-ray Diffraction Results for Liquid-Crystalline Polymers

polymer code	intermolecular spacing, Å	obsd layer spacing, Å	calcd[a] spacing for double-layer packing, Å
PEBP24	4.6	32.0	29.0
PEBP26	4.6	37.0	33.0
PEBP44	4.6	36.0	33.0
PEBP46	4.6	40.0	37.0

[a] The difference between the calculated and observed layer spacings is about 3.5 ± 0.5 Å. This difference is attributed to the uncertain nature of the backbone conformation (a 2/1 helix is assumed) and to the space between chain ends. Turner-Jones has reported[11] a value of 3.3 Å for the space between chain ends in long side-chain poly(1-alkenes).

uted to the uncertain nature of the backbone conformation and to the space between chain ends. Turner-Jones has reported[11] a value of 3.3 Å for the space between chain ends in long side-chain poly(1-alkene)s.

The liquid-crystalline polymers are highly isotactic so a helical backbone conformation seems most likely. Meridional arcs were not observed in the fiber X-ray diffraction patterns, so a determination of the fiber repeat distance could not be made. Turner-Jones has suggested[11] a distorted 3/1 or 4/1 helical structure for long side-chain poly(1-alkene)s. A similar helical structure for the polymers prepared in the present work is probable.

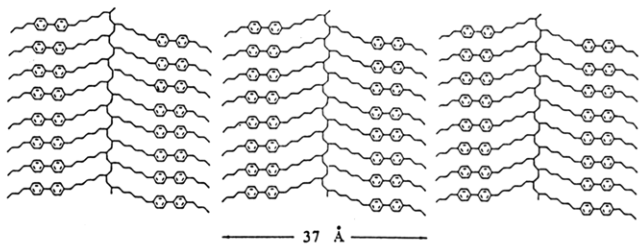

Figure 13. Double-layer packing and calculated layer thickness of PEBP46 is illustrated. The actual layer spacing derived from X-ray diffraction is 40 Å.

The liquid-crystalline polymers at room temperature appear to be smectic E liquid-crystalline glasses.[24] No evidence of crystallinity was observed by X-ray diffraction for any of the liquid-crystalline polymers. Since glass transitions were not detected by DSC, the amount of glassy polymer is probably very low. Although the polymers appeared to soften at 60 ± 5 °C, polymer fibers remained highly ordered even when held for hours at temperatures 10 °C below their respective melting points. The polymers have high molecular weights, and smectic liquid-crystalline phases have high viscosities and resist flow.

The parallels between the polymers prepared for this study and long side-chain poly(1-alkene)s, particularly the well-studied poly(1-eicosene) system, are very interesting. Sluggish transitions between hexagonal and orthorhombic phases appear to be common in both types of polymers. The similarity also extends to the relationship between the liquid-crystalline monomers and linear *n*-alkanes. The liquid-crystalline monomer and model compounds[16] exhibit smectic B and smectic E phases. Linear *n*-alkanes with $n \geq 22$ have been reported[25] to show a hexagonal rotator phase at higher temperatures and more ordered (orthorhombic and triclinic) phases at lower temperatures.

A first-order transition between two thermodynamically stable liquid-crystalline phases would be expected to occur over a more narrow temperature range than that seen in this study and in poly(1-eicosene). One reason for the apparently anomalous behavior is the heating and cooling rates employed in this work. Very slow heating and cooling rates would be expected to define the transition temperatures more clearly. A second reason may be that the relatively inflexible helical backbone present in these polymers does not allow the side chains sufficient mobility for the transition. A third possibility is that the placement of a side group on every other carbon atom of the backbone creates a sterically crowded environment in which side groups are not free to assume new conformations. Magagnini et al. have shown[13] that the hexagonal–orthorhombic transition in poly(1-eicosene) occurs over a broader temperature range than the same transition in poly(octadecylethylene oxide), a polymer that is substituted on every third backbone atom. Some combination of these effects may also be responsible for the broad transitions observed in this work. In any case, the liquid-crystalline polymers prepared in this study seem more closely related to poly(1-alkene)s than to more traditional side-chain liquid-crystalline polymers.

The tacticity of poly(1-eicosene) has been shown[12] to critically affect the transition temperatures. Solvent extraction of the polymers prepared in this study was not successful with boiling hexane, boiling cyclohexane, diethyl ether, room-temperature benzene, and room-temperature toluene in an attempt to remove the small amount of atactic material present. In the second paper

of this series, we reported our attempts to prepare atactic polymer using various catalysts and poly(1-octadecene) as a model system. These experiments produced only oligomeric species.

Another result of this investigation is the dependence of the liquid-crystalline properties on the tail length. For polymers with four- or six-carbon spacers, a two- or four-carbon tail leads to liquid-crystalline behavior. The transition from smectic E to smectic B occurs over a smaller temperature range when a four-carbon tail is present relative to a two-carbon tail. The polymers without tails are not liquid crystalline, and this effect is not due to the length of the side chain. PEBPO6 and PEBP24 have side chains with the same total number of carbon atoms, but only PEBP24 is liquid crystalline.

As reported earlier, the liquid-crystalline properties of the monomers are also highly dependent on tail length. Monoalkyl-substituted biphenyl compounds are not liquid crystalline, and we have suggested[16] that dialkyl substitution of the biphenyl mesogen is a necessary, although not sufficient, condition for liquid crystallinity. The alkyl tail apparently increases the axial ratio of the molecule, thereby enhancing mesogenic behavior. For the monomers, longer tails led to greater mesophase stability, and the same trend is observed for the polymers. The six monomers prepared for this work and a number of other biphenyl liquid crystals have been previously reported.[1-4,16] The liquid-crystalline behavior of these low molecular weight compounds are well established. In contrast, only six hydrocarbon polymers with biphenyl mesogens in the side chain have been prepared in this study, so the conclusions about the relationship between tail length and mesogenic character are more specific and may not be generalized.

The clearing temperatures of the polymers are highly dependent on the spacer length. The clearing temperature of the polymer with a six-carbon spacer is uniformly lower than that of the polymer with a four-carbon spacer. For polymers with the same total side-chain length, such as PEBPO6 vs PEBP24 and PEBP26 vs PEBP44, the polymers with longer spacers also have lower clearing temperatures. The longer spacers apparently increase the flexibility of the side chain, resulting in lower clearing temperatures.

Conclusions

Hydrocarbon polymers containing biphenyl mesogens in the side chain have been synthesized and characterized for the first time. Six new polymers with four- or six-carbon spacers and H, ethyl, or *n*-butyl terminal tail groups were characterized by DSC, X-ray diffraction, and POM measurements. The tail length was found to critically influence the mesophase characteristics of the polymers. Polymers with no tails were not liquid crystalline. The X-ray data showed that the polymers with two- and four-carbon tails were smectic E liquid-crystalline glasses at room temperature. The liquid-crystalline polymers appear to soften at about 60 °C, although no evidence of a glass transition is seen by DSC, probably because there is too little glassy material present. As the liquid-crystalline polymers are heated above 60 °C, X-ray diffraction results show that they undergo a transition from smectic E (orthorhombic packing) liquid-crystalline polymer to smectic B (hexagonal packing) liquid-crystalline polymer. The DSC evidence indicates that the transition occurs over a broad temperature range for the polymers with four-carbon tails. The smectic E to smectic B transition is not detectable by DSC for polymers with two-carbon tails. These results parallel literature data on the crystal structure of poly(1-eicosene). In both cases a orthorhombic–hexagonal transition occurs over a broad temperature range and is undetectable by DSC.

The fiber X-ray diffraction data show that the mesogenic side groups are arrayed on both sides of the backbone, an arrangement known as double-layer packing. Since the polymers are known to be highly isotactic, a helical backbone conformation seems likely, possibly a distorted 3/1 or 4/1 helix. The non-liquid-crystalline polymers, PEBPO4 and PEBPO6, show wide-angle X-ray equatorial arcs for fibers that may result from backbone crystallization. POM investigations of the liquid-crystalline polymers showed fine-grain textures, confirming the smectic phase assignments, whereas the non-liquid-crystalline polymers had nondescriptive textures.

A striking property of the polymers is that a melt-drawn fiber held 1 h at a temperature 10 °C below T_i is found to maintain its highly oriented and ordered state although all polymers soften at ca. 60 °C. This behavior may indicate that the smectic B organization is sufficient to retain a high degree of orientation in the fiber. The thermal and mechanical properties of these materials deserve further attention.

Since only six polymers have been prepared, definitive conclusions cannot be drawn. Further work in this area is needed to confirm the delicate influence of tail and spacer length and particularly tacticity on the liquid-crystalline properties of these new thermotropic hydrocarbon side-chain liquid-crystalline polymers.

Acknowledgment. The support of the National Science Foundation for the Materials Research Laboratory at the University of Massachusetts is gratefully acknowledged. We sincerely appreciate the assistance of Professor T. Atkins, Bristol University, with the interpretation of the X-ray diffraction studies.

References and Notes

(1) Mallon, J. J.; Kantor, S. W. *Mol. Cryst. Liq. Cryst., Inc. Nonlin. Opt.* **1988**, *157*, 25.
(2) Mallon, J. J.; Kantor, S. W. *Mol. Cryst. Liq. Cryst., Inc. Nonlin. Opt.* **1988**, *157*, 43.
(3) Osman, M. A. *Z. Naturforsch.* **1983**, *38A*, 693.
(4) Toyne, K. J. In *Thermotropic Liquid Crystals*; Gray, G. W., Ed.; John Wiley and Sons: New York, 1987; Chapter 2.4.
(5) Samulski, E. T.; Toriumi, H. *Mol. Cryst. Liq. Cryst.* **1983**, *101*, 163.
(6) Petrzilka, M. *Mol. Cryst. Liq. Cryst.* **1984**, *111*, 347.
(7) Takatsu, H.; Takeuchi, K.; Sato, H. *Mol. Cryst. Liq. Cryst.* **1984**, *111*, 311.
(8) Eidenschink, R. *Mol. Cryst. Liq. Cryst.* **1983**, *94*, 119.
(9) Varech, D.; Jacques, J. *Mol. Cryst. Liq. Cryst., Lett. Sect.* **1983**, *92*, 141.
(10) Plate, N. A.; Shibaev, V. P. *Comb Shaped Polymers and Liquid Crystals*; Plenum Press: New York, 1987.
(11) Turner-Jones, A. *Makromol. Chem.* **1964**, *71*, 1.
(12) Magagnini, P. O.; Segre, A. L.; Andruzzi, F.; Lupinacci, D. *Macromolecules* **1981**, *14*, 1845.
(13) Magagnini, P. O.; Andruzzi, F.; Vergamini, P.; Benedetti, E. *Polym. Bull.* **1980**, *2*, 241.
(14) Magagnini, P. O.; Andruzzi, F.; Benetti, G. F. *Macromolecules* **1980**, *13*, 12.
(15) Magagnini, P. O.; Andruzzi, F.; Lupinacci, D.; Paci, M. *Polymer* **1982**, *23*, 277.
(16) Mallon, J. J.; Kantor, S. W. *Macromolecules* **1989**, *22*, 2070.
(17) Mallon, J. J.; Kantor, S. W. *Macromolecules* **1989**, *22*, 2077.
(18) Griffin, A. C.; Haven, S. J. *J. Polym. Sci., Polym. Phys. Ed.* **1981**, *19*, 951.
(19) Roviello, A.; Sirigu, A. *J. Polym. Sci., Polym. Lett. Ed.* **1975**, *13*, 455.
(20) Finkelmann, H.; Rehage, G. In *Advances in Polymer Science 60/61*; Springer-Verlag: Berlin, Heidelberg, FRG, 1984; p 147.
(21) Shibaev, V. P.; Plate, N. A. In *Advances in Polymer Science 60/61*; Springer-Verlag: Berlin, Heidelberg, FRG, 1984; p 193.

(22) Finkelmann, H.; Rehage, G. In *Advances in Polymer Science 60/61*; Springer-Verlag: Berlin, Heidelberg, FRG, 1984; pp 148–49.
(23) Shibaev, V. P.; Plate, N. A. In *Advances in Polymer Science 60/61*; Springer-Verlag: Berlin, Heidelberg, FRG, 1984; p 197.
(24) Wunderlich, B.; Grebowicz, J. In *Advances in Polymer Science 60/61*; Springer-Verlag: Berlin, Heidelberg, FRG, 1984; p 1.
(25) Denicol, I.; Doucet, J.; Craievich, A. F. *J. Chem. Phys.* **1983**, *78* (3), 1465.

Registry No. PEBP04 (homopolymer), 115181-06-1; PEBP06 (homopolymer), 115181-08-3; PEBP24 (homopolymer), 118798-37-1; PEBP26 (homopolymer), 115181-10-7; PEBP44 (homopolymer), 115181-12-9; PEBP46 (homopolymer), 115181-14-1.

Ionic Conductivity in Organic Solids Derived from Amorphous Macromolecules

D. G. H. Ballard,* P. Cheshire, T. S. Mann, and J. E. Przeworski

ICI C&P Ltd, P.O. Box 13, The Heath, Runcorn Cheshire, WA7 4QF, England.
Received April 10, 1989; Revised Manuscript Received July 18, 1989

ABSTRACT: By use of principles derived from the study of the effect of copolymerization on crystallinity and lamellae thickness in semicrystalline systems, amorphous polymers of ethylene oxide have been synthesized. It has been shown that the ionic conductivity in the presence of lithium triflate at room temperatures is significantly improved in these completely amorphous materials, provided the comonomer used has the same C:O ratio as poly(ethylene oxide). The optimum conductivity at 25 °C achieved was on the order of 2×10^{-5} Ω^{-1} cm^{-1} compared to 5×10^{-8} Ω^{-1} cm^{-1} for semicrystalline PEO. The mechanical properties were, however, poor. Amorphous terpolymers were synthesized with the same composition but containing 5% of cross-linkable sites. The effect of cross-linking was to reduce the conductivity by an order of magnitude. However, mechanical properties were good. Studies of a model system dimethoxyethane with propylene carbonate showed that conductivities on the order of 10^{-2} Ω^{-1} cm^{-1} were possible in organic media with lithium triflate. Extension of this concept to the amorphous cross-linked PEO systems showed that the addition of 50% propylene carbonate gave a flexible film with good mechanical properties and a conductivity of 10^{-3} Ω^{-1} cm^{-1}, the highest so far achieved. The use of the latter in the design of eletrochemical cells is discussed.

Introduction

The field of ionically conducting polymer electrolytes has recently attracted a great deal of interest.[1-12] This has mainly been due to their *potential* use in high energy density, solid-state batteries.[3-7] Also, more recently other possible applications have been identified. These include electrochemical displays, proton conductors, and sensors.

Polymer electrolytes are produced from polymers containing polar groups in which are dissolved a salt, usually of an alkali metal (e.g., lithium), and a "soft" anion (e.g., perchlorate). The most studied system in the literature has been poly(ethylene oxide) (PEO) in which LiX ($X^- = ClO_4^-$ or $CF_3SO_3^-$) has been dissolved. However, this material suffers from the disadvantage of forming a partially crystalline polymer–salt complex at room temperature, resulting in a multiphase system, which complicates its study. Such systems only have acceptable conductivities at temperatures in excess of 100 °C.

The view has often been stated in the literature that whatever the mechanism of ion transport in the PEO matrix, the amorphous phase only is involved.[8] However, no systematic study has been attempted to prove this observation. The reason for this is that polymer scientists do not have a clear idea of how to produce amorphous materials from monomers that normally form semicrystalline materials.

The objective of this work was to produce a stable amorphous polymer of PEO in which the ratio of carbon atoms to oxygen atoms was similiar to that in PEO. The principles involved in producing an amorphous polymer from monomers that normally polymerize to give crystallizable polymers has been the subject of a recent study in these laboratories and will be reported in detail in a separate publication.[15] However, some aspects of this work have been discussed in relation to the crystallinity of PVC[13] and polyethylene copolymers.[14] The principles involved are as follows.

(a) A comonomer unit must be chosen such that the side chain formed on copolymerizing with ethylene oxide is too large to enter the crystal lattice of poly(ethylene oxide).

(b) It follows from (a) that in a random copolymerization the distance between comonomer units will determine the average thickness of the lamellae crystals formed by chain folding.

(c) If the thickness of the lamellae is reduced below 30 Å, then, because of thermal motions of the crystallizable molecular fragments, crystallization is not possible and an amorphous structure results.

Our studies of the polyethylene, nylon, PTFE, PEO, PET, and other systems show that (a), (b), and (c) are general principles.

Experimental Section

(a) Synthesis. (i) Monomers. The glycidyl ethers were prepared by using a two-stage synthesis via the chlorohydrin.[16] They were purified by fractional vacuum distillation and their purity was checked by gas chromatography. Only material of

* To whom correspondence should be addressed.

0024-9297/90/2223-1256$02.50/0